environmental sciences proceedings

MDPI

Proceeding Paper

Estimating Permafrost Active Layer Thickness (ALT) Biogeography over the Arctic Tundra †

Emiliana Valentini [1], Marco Salvadore [2], Serena Sapio [2], Roberto Salzano [3], Giovanni Bormidoni [1], Andrea Taramelli [2] and Rosamaria Salvatori [1]

[1] National Research Council of Italy, Institute of Polar Sciences (CNR ISP), postcode City, Country; email1@email.com (E.V.); email2@email.com (G.B.); email3@email.com (R.S.)
[2] University Institute for Advanced Studies of Pavia (IUSS), postcode City, Country; email4@email.com (M.S.); email5@email.com (S.S.); email6@email.com (A.T.)
[3] National Research Council, Institute of Atmospheric Pollution Research (CNR IIA), postcode City, Country; email6@email.com
* Correspondence: email@email.com
† Presented at the 5th International Electronic Conference on Remote Sensing, 7–21 November 2023; Available online: https://ecrs2023.sciforum.net/.

Abstract: The geospatial model here presented estimates the permafrost Active Layer Thickness (ALT) over the entire Arctic in the last 20 years and it is based on the spatial and temporal oscillations measured by satellite-based essential variables associated with the thermal state of permafrost. The model integrates the climate and soil components such as the land surface temperature, the Snow Depth Water Equivalent and the mid-summer albedo, with the structural and functional descriptors of Arctic tundra biome such as the fraction of absorbed photosynthetically active radiation. The distribution of estimated ALT varies according to the vegetation classes (mosses and lichens or grasses and shrubs), but a general increase has been estimated across the whole Arctic tundra region with rates of up to 2 cm/year.

Keywords: permafrost; active layer; model; Arctic amplification; tundra; greening

Citation: Valentini, E.; Salvadore, M.; Sapio, S.; Salzano, R.; Bormidoni, G.; Taramelli, A.; Salvatori, R. Estimating Permafrost Active Layer Thickness (ALT) Biogeography over the Arctic Tundra. *Environ. Sci. Proc.* **2023**, *27*, x. https://doi.org/10.3390/xxxxx

Academic Editor(s): Name

Published: date

1. Introduction

Permafrost, defined as perennially frozen soil, extends over 15% of the Earth's surface exposed in the northern hemisphere and over the entire Arctic and sub-Arctic region (Obu, 2021). The layer above of the permafrost is defined as 'active layer' as it freezes in winter and gradually melts in summer, for a resulting thickness that has been estimated to increase as a function of climate change (Meredith et al., 2019; Trofaier et al., 2017). A recent and wide interest has been dedicated to permafrost and to changes that it undergoes due to global warming (Biskaborn et al., 2019; Romanovsky et al., 2010). The importance of studying the effects of permafrost thawing has been underlined by in 2021 by the European Union in the 'Joint communication on the Arctic and northern dimension policy' for the Arctic Strategy update. The global warming is triggering an earlier snow melting with a consequent lengthening of the snow-off period and of the exposure of land surface to the effect of solar radiation (Trofaier et al., 2017). However, the Land Surface Temperature (LST) has been observed to change with a different rate than the air temperature according to the tundra vegetation cover and the associated mid-summer albedo which is also related to the ALT (Forzieri et al., 2018; Plekhanova et al., 2022). An increase in temperature during the growing season does not necessarily promote plant growth, but rather indicates drought stress caused by the lowering of groundwater levels related to the increase in thaw depth (Opała-Owczarek et al., 2018).

The permafrost freeze/thaw dynamics influence the magnitude of the seasonal vegetation response during the snow-off period and this phenomenon have impacts on permafrost itself (Karlsen et al., 2019). For these reasons, the study of the Thermal State of Permafrost (TSP) and the associated ALT involves several Essential Variables related to vegetation, snow and soil properties (Trofaier et al., 2017).

We present a geospatial model based on Earth Observation (EO) data for estimating biogeographical variation of the permafrost ALT in the Arctic tundra region, over the last twenty years. The model integrates essential variables related to the climate and soil components such as the fraction of the solar radiation absorbed by vegetation for the photosynthesis activity (FAPAR), as a descriptor of Arctic tundra vegetation, because it depends on canopy structures; the Snow Depth Water Equivalent (SDWE) as a proxy of the soil water content, because the winter SDWE is strictly related to the summer soil moisture (Muñoz-Sabater et al., 2021); the albedo as a proxy of the solar radiation reflected back to the atmosphere by land cover which in summer depends on the vegetation cover and the soil saturation (Wang et al., 2019) and the LST, because it directly impacts the thermal state of permafrost (Meredith et al., 2019; Trofaier et al., 2017).

The model develops a holistic approach by weighting the essential variables trends with the in-situ monitoring data from Circumpolar Active Layer Monitoring (CALM) program, which is a component of the Global Terrestrial Network for Permafrost (GTN-P). The result is a set of estimations of ALT over the Arctic tundra biome and as directly related product, the frequency distribution of the green component over the entire period provides the estimation of the greening patterns.

2. Methods

The geospatial model is based on the parametrization of each variable for each pixel within the Region of Interest (Figure 1). For what concern the satellite data, daily MODIS products (NASA) about FAPAR (MOD15A2H V6.1), LST (MOD11A1 V6.1) and Albedo (MCD43A3 V6.1) have been involved as variables in the geospatial model, together with the ERA5 hourly reanalysis of SDWE (ECMWF Climate).

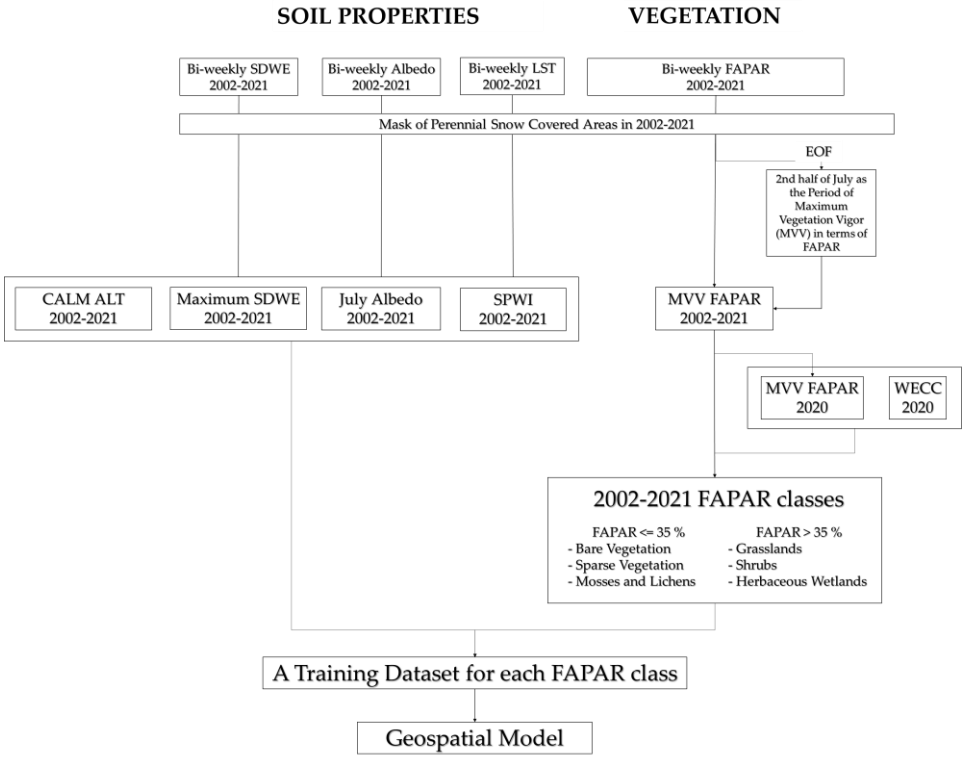

Figure 1. Workflow of the geospatial model for ALT estimations.

Twenty-years (2002–2021) biweekly datasets have been built by considering the average of the MODIS acquisitions in the first and in the last half of each month of the Arctic sun-light period (from March to September) and rescaled at 25 km of spatial resolution. All these datasets have been masked out of the areas covered by ice (from WECC, 2020) and perennial snow. Perennial snow-covered areas have been identified using MODIS data (MOD10A1.061) with a Normalized Difference Snow Index (NDSI) > 0.4 during the whole-time range.

For the Arctic tundra biome classification, the FAPAR dataset has been investigated through the Empirical Orthogonal Analysis (EOF), a statistical technique to rank spatial and temporal patterns of variability, to identify the maximum seasonal vigor period of the Arctic tundra. Then, the FAPAR dataset has been elaborated to obtain a twenty-year yearly dataset considering the average in the maximum seasonal vigor period previously identified. By overlapping the FAPAR values for the year 2020 with the World ESA Land Cover Classification (WECC, 2020), 2 subzones have been obtained.

For soil properties, the LST dataset has been further elaborated to obtain the yearly Sun-Light Period Warmth Index (SPWI) meant as the cumulative sum of the LST monthly means in the sun-light period, while the SDWE and albedo datasets have been elaborated to obtain respectively the yearly Maximum value of SDWE (MDWE) and the July Albedo average (JAlbedo).

Regarding the geospatial model for the estimation of ALT biogeographical variability, it is obtained by building a linear regression model between the yearly SPWI, MDWE and JAlbedo, and the ALT field data provided by the CALM for each subzone.

These variables contribute with different weights in the two FAPAR subzones considering the degree of correlation among the variables that generate 2 sets of coefficients.

The resulting model produced a twenty-years ALT dataset for the Arctic tundra region, and it has been validated through a normal cross-validation, considering the average difference between the estimates and the ground-truth represented by CALM measurements, and a spatial cross-validation considering five zones taken by the CALM sites: West Siberia, East Siberia, Alaska, Canada, and Greenland & Svalbard. The ALT dataset has been further elaborated to extrapolate the estimated rate of change in the 2002–2021.

3. Results and Discussion

Regarding the Arctic tundra classification, the Expansion Coefficients (ECs) from EOFs show an oscillation pattern for which the FAPAR maximum values and the related maximum vegetation vigor in the period 2002–2021 have been reached in the second half of July. This temporal pattern shows also that the FAPAR average observed in the Arctic tundra region starts to increase in April, as until March the majority of Arctic surface is covered by snow, and decreases in August (Meredith et al., 2019). From the analysis of the maximum vegetation vigor (FAPAR maximum values) within the ESA World Cover Classification, two classes have been identified using a threshold of 35% (Figure 2). FAPAR lower than 35% represents areas covered by mosses and lichens and sparse vegetation (Subzone A), while areas above this threshold represents herbaceous cover (Subzone B) (Figure 3a). The resulting FAPAR classes for the year 2003 have been overlapped with the CAVM map of the same year with an overall accuracy of 71%).

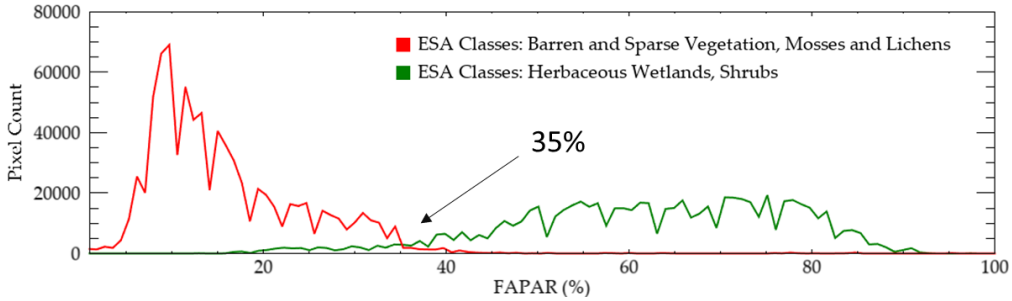

Figure 2. The distribution of FAPAR values in of the two classes of land cover obtained by merging the ESA Land Cover 2020 classes.

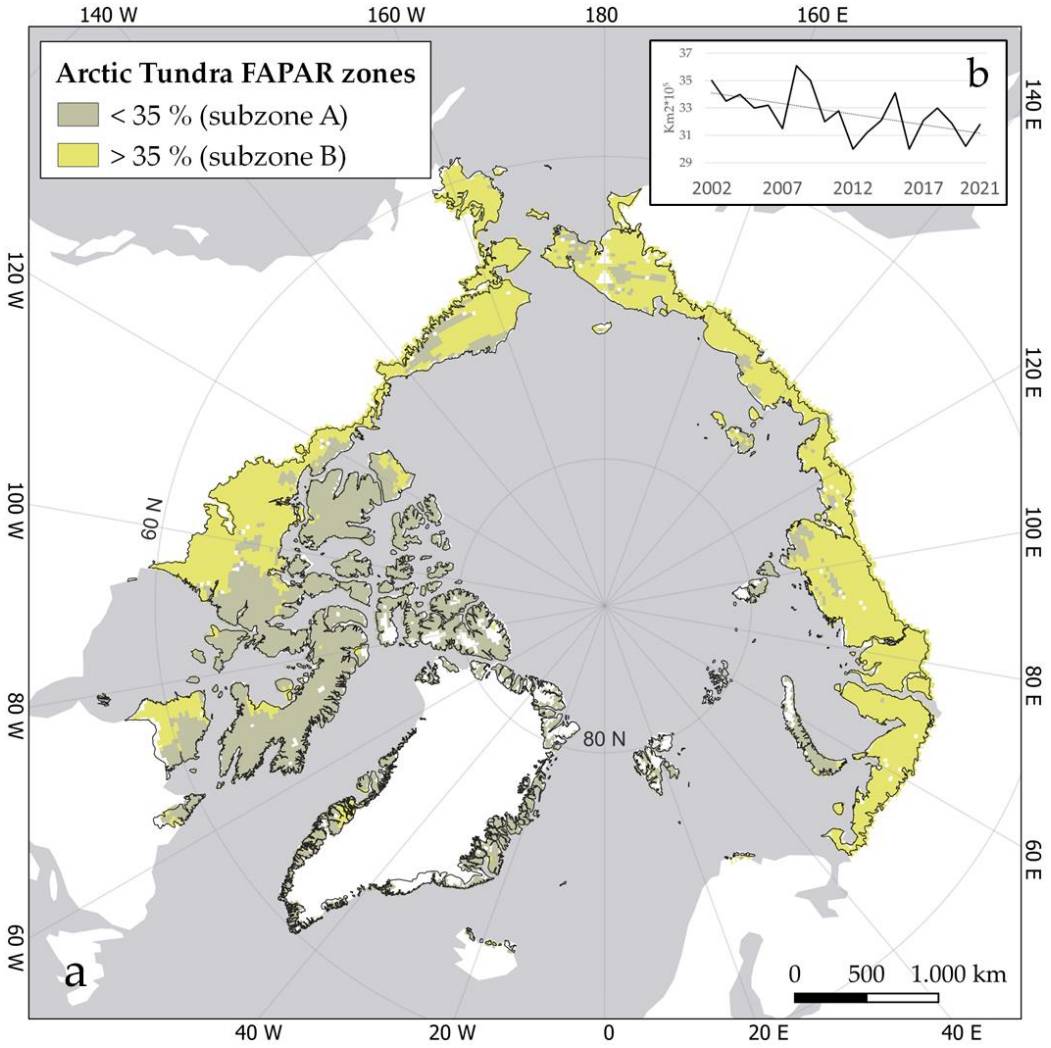

Figure 3. (**a**) The two Arctic Tundra vegetation subzones according to the FAPAR threshold of 35%: mosses and lichens and sparse vegetation < 35% (Subzone A), herbaceous cover > 35% (Subzone B); (**b**) the oscillation of subzone A surface (km^2 × 10^5) over the period 2002–2021 with a dotted line representing the linear intercept of the frequency distribution.

The surface of FAPAR Subzone A over the 20 years highlighted a potential progressive reduction (Figure 3b) probably related to the lengthening of the snow off period and to the ephemeral cycle of this kind of vegetation. This trend could also be explained by the associated Fractional Vegetation Cover (FVC). In fact, a lower FVC, typical of the sparse vegetation of high latitudes, could reduce the average FAPAR reported by the mixed pixels.

The model training phase identify the coefficients associated with the independent variables related to the soil properties respectively for the subzone A (Equation (1)), and the subzone B (Equation (2)) for the following resulting equations:

$$ALT = 57.59 \times \mathrm{M}SDWE + 22.72 \times \mathrm{J}Albedo + 4.13 \times SPWI + 28.14 \quad (1)$$

$$ALT = 54.85 \times \mathrm{M}SDWE + 41.73 \times \mathrm{J}Albedo + 3.06 \times SPWI + 35.03 \quad (2)$$

In Equation (1) are presented the model coefficients obtained from the parametrization for Subzone A, covered by mosses-lichens—sparse vegetation (FAPAR <= 35%; R-squared = 0.51) and in the Equation (2) there are the model coefficients obtained for

Subzone B covered by grasslands—herbaceous wetlands (FAPAR > 35%; R-squared = 0.22). The weight of the MDWE and SPWI in the subzone B is lower than in the subzone A. As for MDWE this difference could be because the snowpack is thicker in the areas represented in the subzone A and, in turn, also the potential water that would come from snow melting and the related impact on ALT is greater than in the subzone B. For what concerns the SPWI, the difference between the weights in the two equations could be explained by the vegetation type, which is more structured in the subzone B and then it could better mitigate the temperature impact on the ALT.

Regarding the weight associated with the JAlbedo, the weight in the Equation (2) is greater than the weight of Equation (1) probably because of the different vegetation typologies represented in the two subzones: the more structural vegetation estimated in the subzone B could lead to a resulting lower JAlbedo which, in turn, could lead to a greater solar radiation absorption impacting more the thermal state of permafrost and the resulting ALT.

The model output is an annual Arctic tundra ALT estimate. As for the accuracy of the result, the cross-validation indicated an error of 9 cm in the Subzone A and of 8 cm of the Subzone B. The spatial cross-validation underlined how in the subzone A, the resulting estimates have a significant uncertanty in Greenland and Svalbard, while in the subzone B, the error is equally distributed over the whole dataset. In the Scandinavian control points, the average error is greater than 15 cm. This error could be due to the lower number of CALM ALT mesurements available for the model training. The increases in 20 years show biogeographical patterns spanning from Alaska, with changes up to 60 cm (from 1 m depth in 2002 to 1.6 m in 2021) to Canada with changes up to 25 cm (from 0.8 m depth in 2002 to 1.05 m in 2021) and Siberia with changes up to 50 cm (from 0.45 m depth in 2002 to 0.95 m in 2021). The resulting ALT spatial distribution shows a general increase over the whole tundra region with rates up to around 2 cm/year (Figure 4).

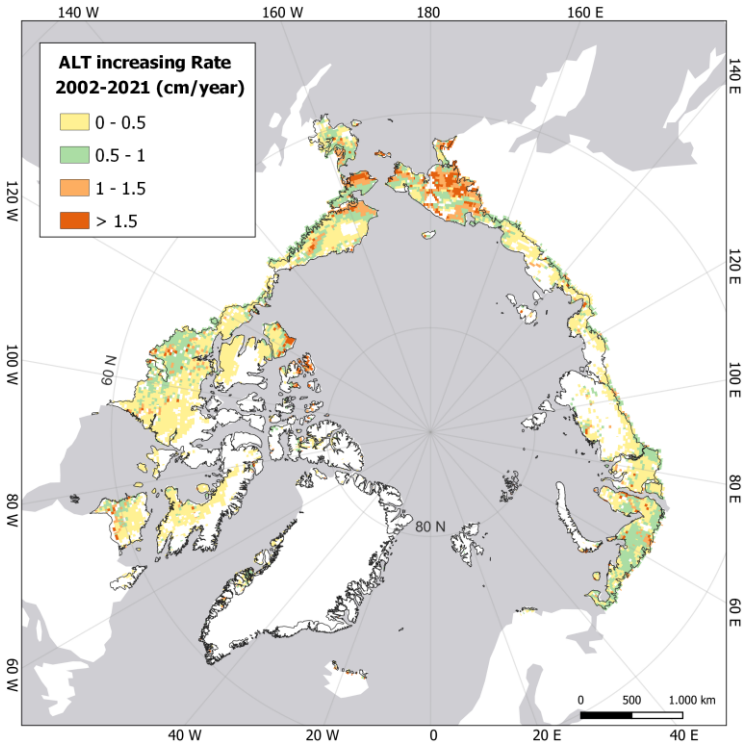

Figure 4. ALT increasing rate calculated as the trend slopes of the linear regression between ALT values and time.

4. Conclusions

The design of the geospatial model here presented, demonstrate the opportunity of integrating functional and structural descriptors of vegetation such as FAPAR with the other essential variables to estimate the biogeographic variability of the ALT in the last 20 years. In these terms, the first outcome of the study is the FAPAR classification associated to the vegetation classes, which allows to confirm the importance of the FAPAR as a descriptor of vegetation typologies but also to open to its application in the High Arctic regions. Furthermore, the identification of the two subzones allows to discuss the differences estimated between the weights of each variable involved in the model and then to investigate the relationships between these variables and the vegetation. The progressive reduction of areas covered by mosses and lichens and sparse vegetation (Subzone A), in favor of the grasses and shrubs cover (subzone B) could decrease the average albedo, leading to an increase in the solar radiation absorption with climate feedbacks effects. The model biogeographical variability highlights some hotspot of ALT, as Alaska, eastern and western Arctic Siberia, and the southern Arctic Canada.

Author Contributions:.

Funding:

Institutional Review Board Statement:

Informed Consent Statement:

Data Availability Statement:

Conflicts of Interest:

References

1. Biskaborn, B.K.; Smith, S.L.; Noetzli, J.; Matthes, H.; Vieira, G.; Streletskiy, D.A.; Schoeneich, P.; Romanovsky, V.E.; Lewkowicz, A.G.; Abramov, A.; et al. Permafrost is warming at a global scale. *Nat. Commun.* **2019**, *10*, 264. https://doi.org/10.1038/s41467-018-08240-4.
2. Forzieri, G.; Alkama, R.; Miralles, D.G.; Cescatti, A. Response to Comment on "Satellites reveal contrasting responses of regional climate to the widespread greening of Earth". *Science* **2018**, *360*, 1180–1184. https://doi.org/10.1126/science.aap9664.
3. Karlsen, S.R.; Stendardi, L.; Nilsen, L.; Malnes, E.; Eklundh, L.; Julitta, T.; Burkart, A.; Tømmervik, H. Sentinel satellite-based mapping of plant productivity in relation to snow duration and time of green-up (GROWTH). In *SESS Report 2019. The State of Environmental Science in Svalbard—An Annual Report*; SIOS: Longyearbyen, Norway, 2019; Volume 9296, pp. 42–57. Available online: https://www.sios-svalbard.org/sites/sios-svalbard.org/files/common/SESSreport_2019_FullReport-150ppi.pdf (accessed on).
4. Meredith, M.; Sommerkorn, M.; Cassotta, S.; Derksen, C.; Ekaykin, A.; Hollowed, A.; Kofinas, G.; Mackintosh, A.; Melbourne-Thomas, J.; Muelbert, M.M.C.; et al. Polar regions. In *IPCC Special Report on the Ocean and Cryosphere in a Changing Climate*, *SUPPL*; IPCC: Geneva, Switzerland, 2019. https://doi.org/10.1016/S1366-7017(01)00066-6.
5. Obu, J. How Much of the Earth's Surface is Underlain by Permafrost? *J. Geophys. Res. Earth Surf.* **2021**, *126*, 1–5. https://doi.org/10.1029/2021JF006123.
6. Opała-Owczarek, M.; Pirożnikow, E.; Owczarek, P.; Szymański, W.; Luks, B.; Kępski, D.; Szymanowski, M.; Wojtuń, B.; Migała, K. The influence of abiotic factors on the growth of two vascular plant species (Saxifraga oppositifolia and Salix polaris) in the High Arctic. *Catena* **2018**, *163*, 219–232. https://doi.org/10.1016/j.catena.2017.12.018.
7. Plekhanova, E.; Kim, J.-S.; Oehri, J.; Erb, A.; Schaaf, C.; Schaepman-Strub, G. Mid-summer snow-free albedo across the Arctic tundra was mostly stable or increased over the past two decades. *Environ. Res. Lett.* **2022**, *17*, 124026. https://doi.org/10.1088/1748-9326/aca5a1.
8. Romanovsky, V.E.; Drozdov, D.S.; Oberman, N.G.; Malkova, G.V.; Kholodov, A.L.; Marchenko, S.S.; Moskalenko, N.G.; Sergeev, D.O.; Ukraintseva, N.G.; Abramov, A.A.; et al. Thermal state of permafrost in Russia. *Permafr. Periglac. Process.* **2010**, *21*, 136–155. https://doi.org/10.1002/ppp.683.
9. Trofaier, A.M.; Westermann, S.; Bartsch, A. Progress in space-borne studies of permafrost for climate science: Towards a multi-ECV approach. *Remote. Sens. Environ.* **2017**, *203*, 55–70. https://doi.org/10.1016/j.rse.2017.05.021.
10. Wang, Z.; Kim, Y.; Seo, H.; Um, M.-J.; Mao, J. Permafrost response to vegetation greenness variation in the Arctic tundra through positive feedback in surface air temperature and snow cover. *Environ. Res. Lett.* **2019**, *14*, 044024. https://doi.org/10.1088/1748-9326/ab0839.